Design of an electro-mechanical portable system using natural human body movements for electricity generation

Sylvie Turri, Dominique Miller, Hamid Ben Ahmed, Bernard Multon

Design of an electro-mechanical portable system using natural human body movements for electricity generation

S. Turri, D. Miller, H. Ben Ahmed, B. Multon

SATIE UMR CNRS 8029 - Brittany Branch, ENS de Cachan - Ker Lann Campus
35170 Bruz - France

e-mail: Sylvie.Turri@bretagne.ens-cachan.fr

Abstract:

In this article, the authors present the energy potential associated with an electromechanical resonant generator that uses natural movements of the human body during walking motion, as a means of increasing the autonomy of portable electronic systems. The article begins by characterizing the human walk in terms of frequency and hip displacement amplitude. A combined mechanical and electrical study is then conducted in order to determine an order of magnitude for recoverable power.

Keywords: *electromechanical resonant generator, direct-drive generator, human energy, portable generator.*

1. Introduction

Portable electrical or electronic systems constitute a very strong growth market. The energy consumption of such devices depends on their functional features (lighting, radio-frequency transmission, calculators, etc.). Despite advances made with respect to component consumption and accumulator capacity, increases in the number of functions have not confirmed the announced major fall in energy needs. Over the past ten-year period, a new outlook has been forged: the direct supply of portable systems from renewable energy available within the human environment.

The mechanical energy produced during human movement, along the same lines as heat emitted and light received, has been studied with considerable interest [1],[2],[3].

As regards the movements that may serve to produce energy, two categories stand out:
- movements performed naturally, which unfortunately place heavy constraints on the system and, for this reason, have been seldom employed up until now;
- movements performed voluntarily, which introduce the disadvantage of requiring the individual to remain in motion throughout the action sequence and which may cause hindrances.

To the best of our knowledge, only certain watches (e.g. "Kinetics" by Seiko) actually make use of natural human movement as a substitute for battery power, yet a watch consumes just very small amounts of energy.

The objective of the present research is to design an electromechanical generator for the purpose of reducing, or even eliminating, dependence on the electrical supply network at the time of accumulator recharging. We will focus more specifically on the use of human body movements. This objective represents a real challenge from the standpoint of energy management, ergonomics and mechatronic technology.

2. The human walk: A natural motion

Although T. Starner [2] demonstrated that the three-dimensional movement of the hip does not constitute the best human energy source, it has been selected for our purposes since mobile devices, such as cell phones, or more generally bags and cases are often carried around the hip.

In considering the human torso as represented in Fig. 1, displacements in the 3 directional components (lateral x, longitudinal y and vertical z) may be recorded thanks to infrared markers [4].

Fig. 2 indicates the 2D hip movement according to components y and z.

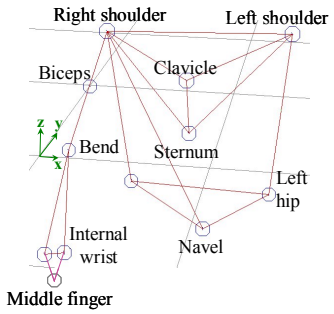

Fig. 1: Marker positions on the walker's bust

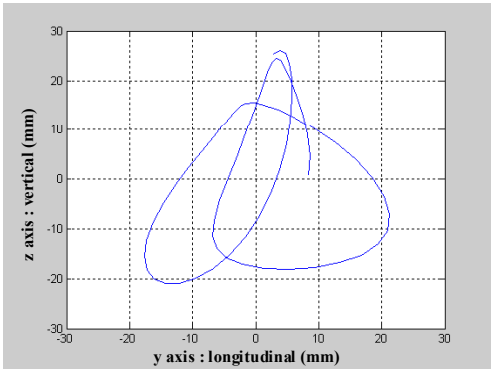

Fig. 2: 2D movements at a walking speed of 5 km/hr (2-step representation)

Depending on the desired components, several types of generators may be designed: rotation using *y* and *z* components (Fig. 2), translation with the *z* component (Fig. 3), etc.

In this article, we propose utilizing the most regular component and the one closest to a sine curve (the vertical component), which is thus easier to employ. Furthermore, a linear generator enables making use of this component by virtue of a very simple mechanical structure.

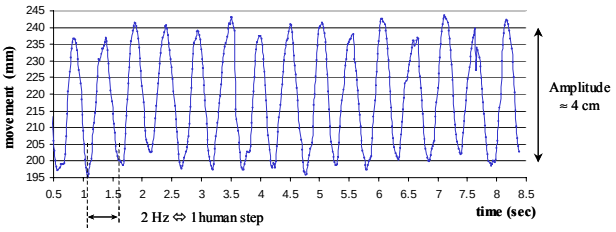

Fig. 3: Vertical right hip movement (*z* component) while walking at 5 km/hr

Given the findings from Fig. 3, we are in a position to consider, within the scope of the present modeling effort, the vertical hip movement as a quasi-sinusoidal source.

$$h(t) = X_M.\cos(\omega_{step}.t) \qquad (1)$$

where X_M equals approximately 2.10^{-2} m and f_{step} lies on the order of 2 Hz, with this latter magnitude varying little from one individual to the next during the course of normal walking.

3. Potential of an electro-mechanical resonant generator

Since the hip movement we selected is quasi-sinusoidal, a significant level of mechanical power will only be recovered by operating very close to a resonance frequency.

This concept has been previously studied in depth for wristwatches and rotary resonators [5], albeit for power ratings of just a few µW [6]. Our goal herein is to reach a power in the several tens of mW.

3.1 Equivalent mechanical structure

Fig. 4 illustrates a mechanical system containing a case incorporated onto the human body by means of a belt fastened around the waist, inside of which a flyweight (to serve as the mobile part of the linear electromechanical generator) suspended between two springs will be in motion, thereby allowing the device to enter into resonance with the hip movement.

According to this simplified diagram (with the thickness of the flyweight being negligible), the amplitude of movement (clearance) is limited by the height of the case. This feature will be modeled by the use of very high-stiffness springs (i.e. stop springs).

This basic configuration allows adopting a simple mechanical approach and remains valid regardless of the final solution chosen (leaf springs, helical springs, rotary springs, etc.).

If the movement were to be studied within a single dimension, the forces applied on the flyweight would be:

- its weight: $P = -m.g$;
- the elastic recoil of the springs, according to the convention established in Fig. 4: $F_R = k.(L - L_0)$, with k being the equivalent stiffness of both springs (k = 2.k');

- an electromagnetic force F_{em} due to the conversion of mechanical energy into electrical energy. Since the electrical generator used is electromagnetic with windings in the airgap (see Section 4), this force will be Laplace in nature and proportional to the current flow. Its sign is always opposite that of the speed (i.e. generator mode, regardless of displacement direction), with $F_{em} = f(i(v))$;
- dry friction;
- viscous friction.

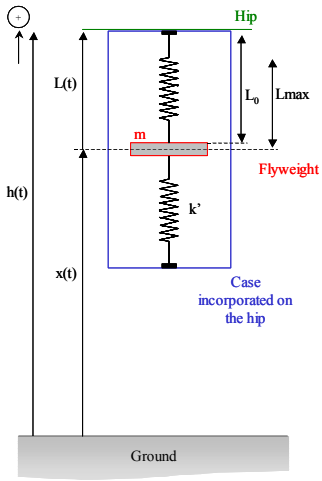

Fig. 4: Mechanical structure of a linear generator

It is thereby possible to write the fundamental mechanical law in neglecting the mechanical friction:

$$\sum F = m.\frac{d^2x(t)}{dt^2} \qquad (2)$$

$$m.\frac{d^2x(t)}{dt^2} = -m.g + k.[L(t) - L_0] + f(i) \qquad (3)$$

with:

m: flyweight mass;
k: spring stiffness;
L(t): length of flyweight displacement;
L_0: initial spring length;
$x(t) = h(t) - L(t)$.

Hence:
$$m.\frac{d^2L(t)}{dt^2} = m.\frac{d^2h(t)}{dt^2} - m.g - f(i) - k.L(t) - k.L_0 \qquad (4)$$

By setting $L_1(t) = L(t) - L_0 - \frac{m}{k}.g$, both the first and second derivatives of $L_1(t)$ remain unchanged and the following may ultimately be obtained:

$$m.\frac{d^2L_1(t)}{dt^2} = m.\frac{d^2h(t)}{dt^2} - f(i) - k.L_1(t) \qquad (5)$$

which generates the model (Matlab-Simulink diagram) shown in Fig. 5. In order to simplify notation, we will hereafter write L(t) instead of $L_1(t)$.

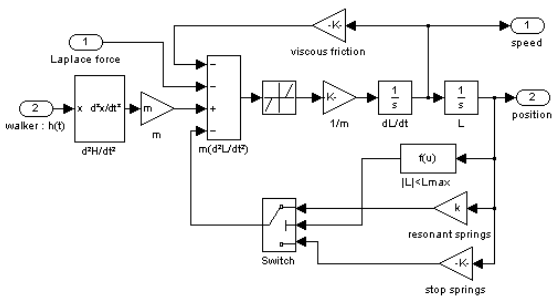

Fig. 5: Mechanical system model

Without drawing any conclusions at this stage regarding either the generator or the converter placed between the generator and the load, it can still be stated that the e.m.f. will depend on both the position and speed of the flyweight. The type of converter and load will impose the law $i = f(u)$, where u is the tension (see Fig. 6).

The general model is presented in Fig. 7. The generator, converter and load compose the electrical system.

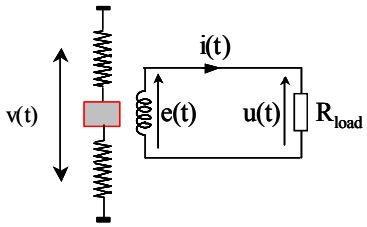

Fig. 6: Diagram of the energy conversion principle

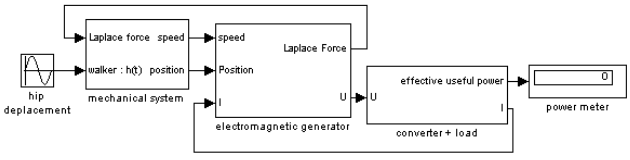

Fig. 7: General electromechanical model

Optimization of the overall assembly will then serve to identify the parameters of each of the two components (mechanical and electromagnetic systems) in order to derive the maximum effective useful power.

As an initial approach however, we have elected to proceed by means of separately optimizing the mechanical and electrical systems (i.e. maximum mechanical power on the one hand, and highest electrical system output on the other), which enables us to determine an order of magnitude for the potential of each system and to subsequently set the initial conditions for an overall optimization.

An analytical study of the mechanical system presupposes knowing the Laplace force f(i) as a function of solely the mechanical magnitudes (i.e. speed, position). It is thereby necessary to forward several hypotheses:

- Given the frequencies involved in this set-up (on the scale of a few hertz) as well as the small dimensions, induction effects have been neglected.
- The e.m.f. is proportional to the speed, and the converter-load assembly imposes a law:
  - either of the type $F_{em} = \lambda \cdot \left(\frac{dL}{dt} \right)^{\alpha}$, with $\alpha = 1$ corresponding to a resistive load;
  - or of the type $F_{em} = \lambda \cdot \frac{dL}{dt}$ for $\left| \frac{dL}{dt} \right| \geq \text{threshold}$, which corresponds to a tension source load through a diode rectifier.

For purposes of illustration (using a small 50-g mass, a resonance frequency of 2 Hz and a peak-to-peak flyweight clearance of 8 cm), we have simulated the expected maximum mechanical power recovered in the absence of both dry friction and viscous friction for the two types of laws described above. Results are shown in Fig. 9 and Fig. 8.

From Fig. 9, it can be observed that the maximum power depends very little upon α beyond a value of 0.5 ($\alpha = 1$ corresponds to a resistive load).

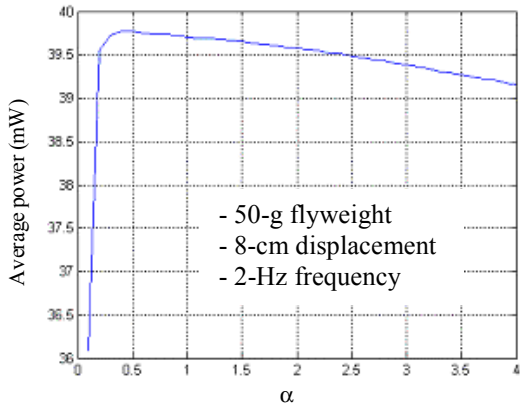

Fig. 8: Maximum average recoverable mechanical power (in mW) as a function of α for $F_{em} = \lambda \cdot \left(\frac{dL}{dt} \right)^{\alpha}$

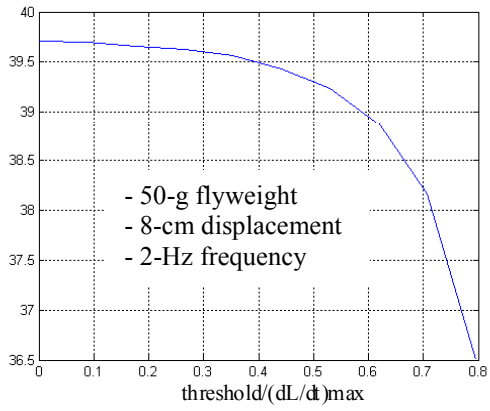

Fig. 9: Maximum average recoverable mechanical power, in mW, as a function of the threshold, where: $F_{em} = \lambda \cdot \frac{dL}{dt}$ for $\left| \frac{dL}{dt} \right| \geq \text{threshold}$

Fig. 8 reveals that the presence of a threshold, below which the generator no longer provides output, is always detrimental.

Regardless of the individual case, it is therefore advantageous to consider that the Laplace force yields a viscous friction, i.e. the converter and load together behave like a resistance (adaptable, in order to obtain optimal operations). The mechanical system is hence a second-order linear system whose behavior can be predetermined with precision.

3.2 Mechanical-electrical analogy

The basic equation for this analogy is as follows:

$$m.\frac{d^2L(t)}{dt^2} = m.\frac{d^2h(t)}{dt^2} - \lambda \cdot \frac{dL}{dt} - k.L(t) \qquad (6)$$

where $h(t) = X_m \sin(\omega_{step} \cdot t)$. The resonance frequency of the unconstrained system is: $\omega_0 = \sqrt{\frac{k}{m}}$.

The expression: $$F_M = m.X_M.\omega^2 \quad (7)$$

describes the amplitude of the sinusoidal excitation applied to the system. An equivalent electrical model (see Fig. 10) can be set up, whereby the transferred power is equal to that dissipated in the resistance R, hence $R \cdot i^2$, equivalent to $\lambda \cdot \left(\frac{dL}{dt}\right)^2$, with: $$\frac{dL(t)}{dt} = \frac{\omega_{step}.F_M.\cos(\omega_{step}.t)}{\lambda.\omega_{step} + j.(m.\omega_{step}^2 - k)} \quad (8)$$

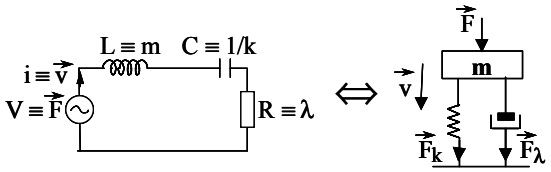

Fig. 10: Equivalent mechanical and electrical models

3.3 Operations at resonance

Mechanical power is obviously maximized at resonance, i.e. for a value $\omega_{step} = \omega_0 = \sqrt{\frac{k}{m}}$ and equals: $P_{max} = \frac{F_M^2}{2.\lambda}$.

For a given excitation F_M, the constant λ enables recovering the desired level of power; in this case however, the speed and hence clearance must be allowed to increase as high as necessary. If the stop springs were assimilated with very stiff springs, the power would drop once these springs have been reached (Fig. 11 highlights the evolution in power vs. λ for a 50-g flyweight and 4 or 8-cm clearances).

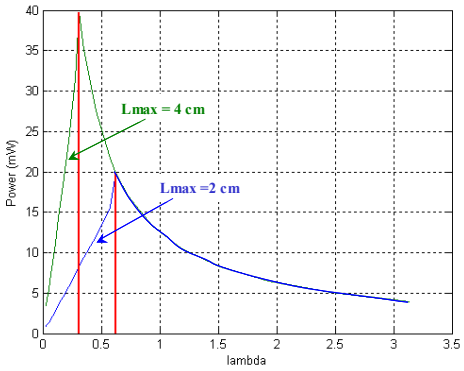

Fig. 11: Influence of a limited clearance on the mechanical power

Let L_{max} represent the maximum displacement of the flyweight towards either the top or bottom from the central position (which will depend upon both the height of the flyweight and the maximum compression of the spring).

It then becomes necessary to determine λ_{opt}, which enables obtaining maximum power for a system equipped with stop springs. The inequality $|L| \le L_{max}$ must always be preserved: $\frac{dL(t)}{dt} = \frac{F_M.\cos(\omega.t)}{\lambda}$,

thus: $$L(t) = \frac{F_M}{\lambda.\omega} \cdot \sin(\omega.t) \quad (9)$$

or: $|L| \le L_{max}$, hence $\frac{F_M}{\lambda.\omega} \le L_{max}$. It then follows that: $\lambda \ge \frac{F_M}{\omega.L_{max}}$. (10)

In our case where h(t) is sinusoidal, maximum power is obtained when reaching the stop spring limit, i.e. for: $$\lambda_{opt} = \frac{m.X_M.\omega}{L_{max}} \quad (11)$$

and ultimately at resonance: $$\boxed{P_{max} = \frac{m.X_M.\omega^3.L_{max}}{2}} \quad (12)$$

This expression yields the maximum recoverable mechanical power. Electrical power will then depend on the output generated from the electricity conversion chain.

The expression of this power with respect to the power due to kinetic energy P_{cin} is given by the following: $P_{max} = \frac{X_M}{L_{max}} \cdot P_{cin}$ with: $P_{cin} = \frac{1}{2} m.\omega^3 .L_{max}^2$ (13)

In considering a 50-g flyweight (with a spring stiffness coefficient at resonance of $k_0 = 7.89\ N.m^{-1}$) and a length $L_{max} = 4$ cm, a maximum average mechanical power of 40 mW is obtained at resonance provided that the load has been adapted such that: $\lambda_{opt} = 0.314$. Fig. 11 also indicates the sensitivity of the system to the value of λ.

3.4 Operations under a varying excitation frequency

Let's now present results for the general case where the resonance frequency of the spring is not necessarily synchronized with that of the walking step.

Let f_{step} be the frequency of the excitation signal and f_0 be the resonance frequency of the mechanical system; the following theoretical relationships can then be written, where $[\omega_{min}, \omega_{max}]$ represents the range of circular walking step frequencies that allow the flyweight to reach the stop springs.

If $\omega_{step} \in [\omega_{min}, \omega_{max}]$, with:

$$\omega_{min} = \frac{\omega_0}{\sqrt{1+\frac{X_m}{\sqrt{2}L_{max}}}}, \omega_{max} = \frac{\omega_0}{\sqrt{1-\frac{X_m}{\sqrt{2}L_{max}}}} \quad (14)$$

then:

$$\begin{cases} P_{max}(\omega_{step}) = \frac{m.\omega_{step}.L_{max}^2}{2} \cdot \sqrt{\left(\frac{\omega_{step}^2.X_M}{L_{max}}\right)^2 - \left(\omega_{step}^2 - \omega_0^2\right)^2} \\ \lambda_{opt}(\omega_{step}) = \frac{m}{\omega_{step}} \cdot \sqrt{\left(\frac{\omega_{step}^2.X_M}{L_{max}}\right)^2 - \left(\omega_{step}^2 - \omega_0^2\right)^2} \end{cases} \text{ else } \begin{cases} P_{max}(\omega_{step}) = \frac{m.X_M^2}{4} \cdot \frac{\omega_{step}^5}{\left|\omega step - \omega_0^2\right|} \\ \lambda_{opt}(\omega_{step}) = m \cdot \frac{\left|\omega_{step}^2 - \omega_0^2\right|}{\omega_{step}} \end{cases}. \quad (15)$$

At resonance $\omega_0 = \omega_{step}$, we are able to write the following:

$$P_{max}(\omega_{step}) = \frac{m.X_M.L_{max}.\omega_{step}^3}{2}, \text{ with: } \lambda_{opt}(\omega_{step}) = \frac{m.X_M.\omega_0}{L_{max}}. \quad (16)$$

Fig. 12 and Fig. 13 display the results derived for a 50-g flyweight and a ± 4-cm clearance.

It can be observed (Fig. 12) that the presence of stop springs serves to considerably limit the recoverable power.

Moreover, as shown in Fig. 13 for a given resonance frequency of the mass-spring system, recovered power increases continuously with walking step frequency. Nonetheless, this power will always remain less than that obtained when the system is synchronized with walking step frequency.

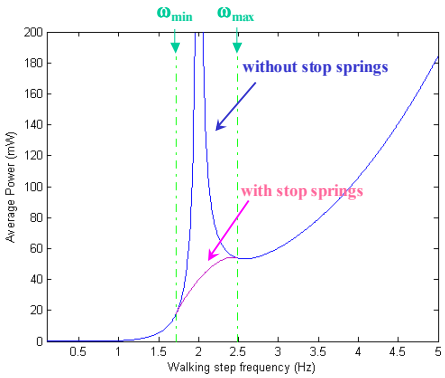

Fig. 12: Average power for $f_0 = 2$ Hz and several walking step frequencies (with and without stops)

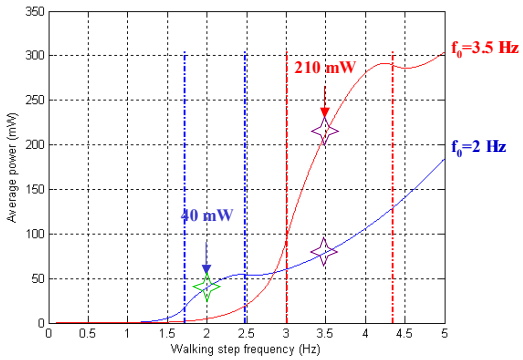

Fig. 13: Average power for $f_0 = 2$ Hz and $f_0 = 3.5$ Hz at several walking step frequencies

3.5 Conclusion

The mechanical power capable of being recovered from a system operating at a frequency close to its resonance depends not only on the mass, but also on the potential clearance. This power is maximized when reaching the stop spring limit, which thereby enables a rather simple mode of regulation.

4. Generator design

4.1 Generator structure

An operating diagram of the electromagnetic structure within the direct linear generator is displayed in Fig. 14 and Fig. 15. The solution presented is not unique and features a mobile winding fastened to the flyweight; we have however envisaged other fixed-winding, mobile-magnet architectures as well.

The flyweight is composed of a laminated ferromagnetic yoke and concentric coils in air organized in single phase winding. The fixed stator, ultimately assembled onto the device case, consists of a neodymium-iron-boron type of radially-magnetized successive rings, along with an external ferromagnetic armature. This set-up provides for an airgap winding machine, which should exhibit minimum detent force.

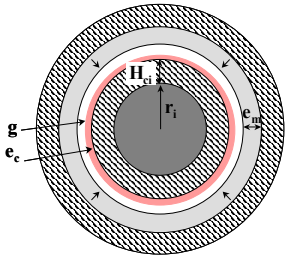

Fig. 15: Transversal section cut of the generator

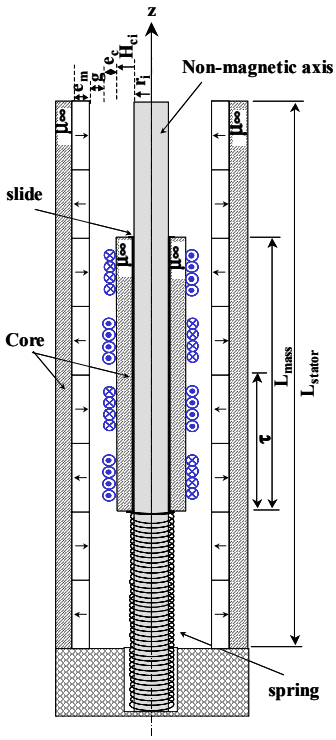

Fig. 14: Simplified generator diagram (longitudinal section cut)

4.2 Design example

Since the device proves to be axisymmetrical, the use of finite elements allows easily determining the induction at the winding level for a given geometry.

Table I: Simulation data

τ	24 mm
L_{mass}	48 mm
L_{stator}	128 mm
e_m	6 mm
g	0.5 mm
e_c	3.5 mm
H_{ci}	10 mm
r_i	0.5 mm
B_r	0.99 T
μ_m	1.01

Fig. 16, derived with the parameters listed in Table I, reveals that this induction may be considered as practically sinusoidal:

$$B_g(z) = B_{gM}.\sin\left(\frac{2.\pi}{\tau}\cdot z\right) \qquad (17)$$

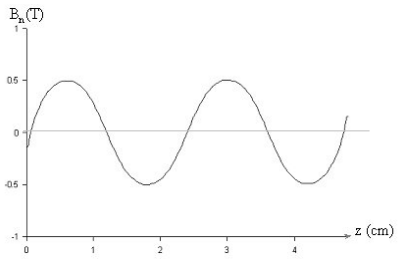

Fig. 16: Induction within the airgap, as determined by use of Finite Elements [7]

The evolution in B_{gM}, as a function of the airgap obtained from Finite Elements [7], is shown in Fig. 17.

For a given polar step and airgap, it is then possible to identify the winding that will yield maximum generator output while still allowing for optimal operations of the mechanical system.
The single phase winding, positioned on the flyweight, is produced by placing n_c coils at a spacing of $\tau/2$ into series. Each coil is composed of n_l layers of n turns wound with a wire of diameter d. Our research has not addressed the connection and has considered that the converter and a temporary storage capacitor will be integrated into the flyweight.

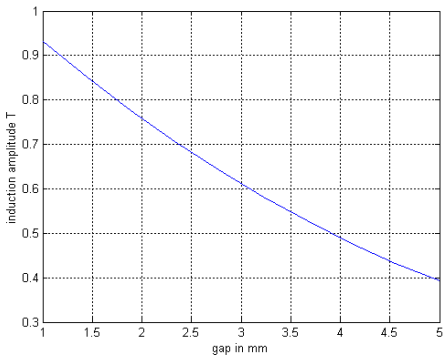

Fig. 17: Induction amplitude vs. magnetic length (e_c+g)

a. E.M.F.

Given that the coils move at speed $v = \frac{dz}{dt}$ (Fig. 18), the electromotive force induced at the terminals of a single turn can be written: $e_c(z) = B_{gM}.ls.\frac{dz}{dt}.\sin\left(\frac{2.\pi}{\tau}\cdot z\right)$ with: $ls = 2.\pi.\left(r_i + H_{ci} + \frac{d}{2}\right)$. (18)

The amplitude of the electromotive force induced at the coil terminals may then be deduced as follows:

$$E_m\left(n, n_l, d, \frac{dz}{dt}\right) = B_{eM}.ls.\frac{dz}{dt}.k_w(n,d) \quad (19)$$

with: $k_w(n,d) = 2.\sum_{n=1}^{N_{max}} \cos\left(\frac{2.\pi}{\tau}\cdot n.d\right)$ and ls being the total length of the turns.

The induced e.m.f. may then be derived:

$$e_m(n, n_l, d, z) = E_m\left(n, n_l, d, \frac{dz}{dt}\right).\sin\left(\frac{2.\pi}{\tau}\cdot z\right) \quad (20)$$

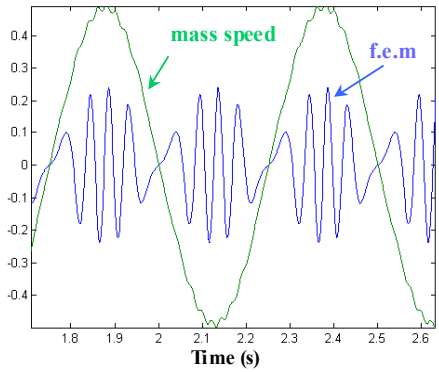

Fig. 18: Shape of the speed profiles and e.m.f. for a sinusoidal flyweight displacement

b. Laplace force

When a coil is crossed by current i, the Laplace force, applied on single phase winding, is expressed as follows:

$$f(n,d,z)\cdot\frac{dz}{dt} = e(n, n_l, d, z).i(z) \quad (21)$$

thus: $$f(n,d,z) = B_{gM}.ls.k_w(n,d).i(n,d,z).\sin\left(\frac{2.\pi}{\tau}\cdot z\right) \quad (22)$$

These expressions then serve to define the electrical system model (see Fig. 19).

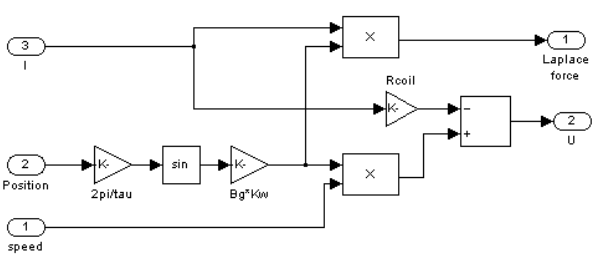

Fig. 19: Electrical model

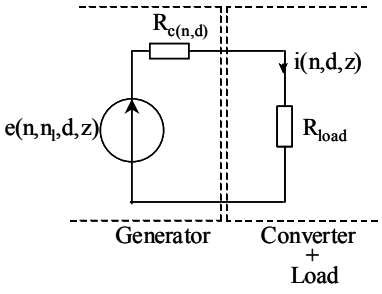

Fig. 20: Electrical diagram

On the resistive load (Fig. 20.), the following may be written: $$i(n,d,z)=\frac{e(n,n_1,d,z)}{R_c(n,d)+R_{load}(n,d)}. \quad (23)$$

Hence: $$f(n,d,z)=\frac{\left(B_{eM}.ls.k_w(n,d)\right)^2.\frac{dz}{dt}}{R_c(n,d)+R_{load}(n,d)}\cdot\sin^2\left(\frac{2.\pi}{\tau}.z\right) \quad (24)$$

The Laplace force is, for constant speed v, a squared sine curve whose average value can be expressed as follows:

$$F(n,d)=\frac{1}{2}\cdot\frac{\left(B_{gM}.ls.k_w(n,d)\right)^2}{R_c(n,d)+R_{load}(n,d)}\cdot v \quad (25)$$

In the case of optimal operations, flyweight displacement is sinusoidal, and maintaining a constant speed proves impossible. Nonetheless, in plotting the course of both the "actual" Laplace force and the steady-state speed for a given configuration (Fig. 21), it can be observed that the same type of operations (small "ripples" at nearly the same speed) is obtained as for the theoretical mechanical system, by expressing the "equivalent" Laplace force in the following form:

$$F=\lambda\cdot v \quad (26)$$

where λ has been extracted from Equation 25.

c. Optimization procedure

From Equations (11) and (12), it has been shown that maximum power will be recovered if:

$$\lambda_{opt}=\frac{1}{2}\cdot\frac{\left(B_{gM}.ls.k_w(n,d)\right)^2}{R_c(n,d)+R_{load}(n,d)}=\frac{m.\omega_0.X_M}{L_{max}} \quad (27)$$

The equivalent optimal resistive load can thus be deduced for a given mechanical configuration:

$$R_{load}(n,d)=\frac{\left(B_{gM}.ls.k_w(n,d)\right)^2}{2.\lambda_{opt}}-R_c(n,d) \quad (28)$$

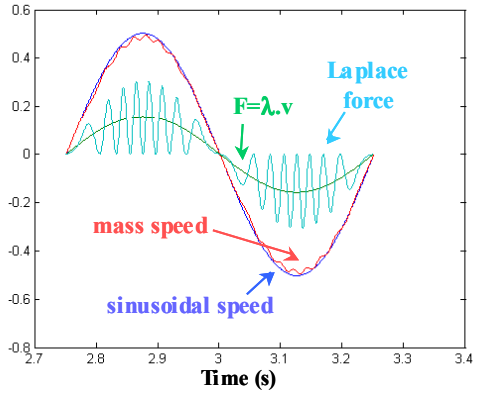

Fig. 21: Actual and equivalent Laplace forces and speeds

Electrical system output is then expressed as: $$\eta(n,n_1,d)=\frac{R_{load}(n,d).i(n,d,z)^2}{e(n,n_1,d,z).i(n,d,z)} \quad (29)$$

with: $$e(n,nl,d,z)=\left[R_c(n,d)+R_{load}(n,d)\right]i(n,d,z) \quad (30)$$

Lastly, output as a function of winding characteristics yields:

$$\eta(n,n_1,d)=\frac{R_{load}(n,d)}{R_c(n,d)+R_{load}(n,d)} \quad (31)$$

The optimization procedure consists of identifying the optimal characteristic magnitudes of the generator (n, n_l, and d) in order to maximize output (Equation 31) for a given mechanical configuration (Equation 11).

The algorithm associated with such a search procedure has been schematized in Fig. 22.

For purposes of illustration, Fig. 23 displays the power supplied (within a pre-established operating mode) to the converter-load assembly in the case of a 2-Hz walking motion for a 50-g flyweight and an 8-cm flyweight displacement.

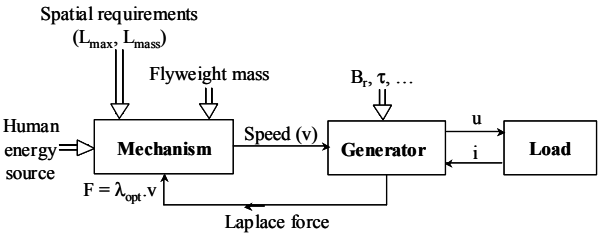

Fig. 22: Optimization flowchart

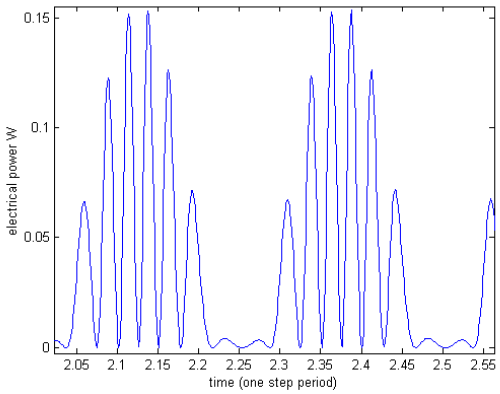

Fig. 23: Example of electrical power at optimal load

5. Conclusion

This article has presented an original, albeit quite simple, system based on a linear generator. A high level of agreement has been obtained between the analytical modeling set-up and results from a simulation that closely replicated the actual system.

The objective of producing several tens of mW is attainable by means of imposing a constant V/I ratio for the load that may be adapted to specific walking conditions. Generator output will rely upon generator optimization including low consumption electronic power converter, which is the topic of ongoing research.

Monitoring the achievement of optimal power recovery proves relatively straightforward, with the goal herein being to extend the mobile part of the device to the stop spring limit.

For the time being, we have not integrated purely-mechanical friction, and in particular that of the flyweight guidance system. Dry friction will not alter the level of recovered power as long as it does not prevent the flyweight from reaching the stop springs. Viscous friction will directly remove a portion of available power. Due to the low displacement speeds, this friction should not attain very high levels. Yet at this stage, only experimental measurements will enable evaluating these frictions in accordance with the technological solutions selected for the guidance system.

6. References

[1] Conference proceedings (in French), "Energie Portable : autonomie et intégration dans l'environnement humain", Club EEA, Cachan, March 2002 (http://www.lesir.ens-cachan.fr/lesir/actualites/actualites.htm).

[2] Starner T., "Human-Powered Wearable Computing", *IBM Systems Journal*, Vol. 35, pp. 618-629, 1996.

[3] Jansen A.J., Stevels A.L.N., "Human Power: A sustainable option for electronics", *Electronics and the Environment, IEEE International Symposium Proceedings*, 1999, pp. 215-218.

[4] Turri S., Multon B., Ben Ahmed H., Miller D., Multon F., Delamarche P., "Caractérisation d'un générateur portable : de l'énergie humaine à l'électricité", GEVIQ 2002, Marseille, June 12-13, pp. 11-16.

[5] http://www.horlogerie-suisse.com, Website.

[6] Born J.J., Dinger R., Farine P.A., "Automatic mechanical movement with quartz precision", Asulab SA, *7th European Congress on Chronometry, Karlsruhe, October 9-10, 1998*.

[7] Meeker D., Finite Element Method Magnetics, femm 3.3, http://femm.berlios.de/.